International Journal of Applied Engineering Research ISSN 0973-4562 Volume 12, Number 17 (2017) pp. 6699-6703

Optimization of Membrane Thickness in Physical Aging Study of Polymeric Membranes

S.S.M. Lock, [a] K.K. Lau, [a*] A.M. Shariff, [a] Y.F. Yeong [a] and F. Ahmad [b]

[a] Research Center for CO_2 Capture, Department of Chemical Engineering, Universiti Teknologi PETRONAS, 32610 Perak Darul Ridzuan, Malaysia.
[b] School of Science and Engineering, Teesside University, Middlesbrough, United Kingdom.
** Corresponding author*
**Orcid ID: 0000-0003-1026-8572*

Abstract

Polymeric membranes are inherently non-equilibrium and experience a naturally occurring progression towards equilibrium, which is regarded as physical aging. It is required to incorporate physical aging phenomena in membrane permeation mechanism to quantify such effect to the separative performance under varying membrane thicknesses. In this work, the densification process within polymeric matrix throughout aging has been simulated through adaptation of the dual mode mechanism, which encompasses the lattice contraction and diffusion of free volume. Later, the dual mode model has been integrated within a succession of states methodology that analytically addresses the separation mechanism in a cocurrent membrane based on the solution-diffusion theory. To the best of our knowledge, this paper is the first pioneering attempt that incorporates the effect of aging on separation performance of membrane. In this study, when membrane thickness is increased from 100 to 400 nm, the initial membrane requirement is also increased by 3.85 times. Nonetheless, the recovery performance after 1 year of aging also reduces from 21.35% to 12.39%. It is found that although the thinner polymeric membrane inherits higher permeance characteristic, making it a highly sought after structure as compared to its bulk counterpart by exhibiting higher driving force and hence smaller area requirement, the thinner membrane also demonstrates drawback of accelerated physical aging, which contributes to higher reduction in product recovery. The optimum membrane thickness has been determined to be 174 nm in present work.

Keywords: Simulation, Thickness, Aging, Gas Separation, Polymer Membrane.

INTRODUCTION

Polymeric membranes have been employed in O_2/ N_2 separation. Nonetheless, they are at glassy and non-equilibrium states, which spontaneously undertake volume relaxation towards equilibrium. The process is commonly known as physical aging. Aging has been proposed to be rationalized through densification of polymeric matrix, which confines the void space for permeability of penetrants [1]. To date, the most widely acknowledged theory that explains physical aging in polymeric membrane is the dual mode mechanism [2], whence it is comprised of i) The size independent "lattice contraction", whereby the free volume throughout the polymeric membrane matrix is subsided homogenously and ii) The size dependent "diffusion of free volume" to surface of the polymer membrane, in which annihilation of free volume occurs at the interfacial layer. Hence, in this work, the dual mode mechanism has been incorporated within a finite element algorithm to model the physical aging process of different membrane thicknesses, whence the membrane is subdivided into many predefined compartments of equal sizes in the thickness direction [3]. Subsequently, the numerical solution has been further implemented within a succession of states methodology that analytically addresses the separation mechanism of a cocurrent membrane. Finally, the mathematical model has been adopted to study the effect of physical aging under varying membrane thicknesses to optimize the parameter employed in air separation. As such, this paper is the first pioneering work that considers the effect of aging on simulation of industrial application through employment of membrane over its lifespan.

METHODOLOGY

Succession of States for Membrane Separation Mechanism

The permeate composition of the component with a higher affinity to pass through a membrane matrix in a binary gas mixture, $y_1[j+1]$, can be calculated using Eq. (1) [4].

$$y_1[j+1]=\frac{(\alpha-1)(\beta x_1[j]+1)+\beta-\left[\left((\alpha-\beta)(\beta x_1[j]+1)+\beta\right)^2-4\alpha\beta x_1[j](\alpha-1)\right]^{0.5}}{2(\alpha\text{-}1)} \quad (1)$$

In Eq. (1), α is the ideal selectivity, which can be deduced as the fraction of time dependent O_2 to N_2 permeability $\left(P_{O_2}(t)/P_{N_2}(t)\right)$, β is the ratio of the pressure $\left(p_h/p_l\right)$, $x_1[j]$ is feed side composition of O_2. By adapting the solution

diffusion model, the overall gas flow that permeates through the membrane, ΔV, and the amount of gas that penetrates through the membrane for each gas species contained with the binary gas, ΔV_n, are calculated from Eq. (2) and Eq. (3) [5].

$$\Delta V = \sum_{n=1}^{N} \left[P_n(t)/l \right] A_m \left(p_h x_n[j] - p_l y_n[j+1] \right) \quad (2)$$

$$\Delta V_n = \left[P_n(t)/l \right] A_m \left(p_h x_n[j] - p_l y_n[j+1] \right); n = 1,2 \quad (3)$$

Whereby $P_n(t)$ is the time dependent permeability of each component, l is thickness of the membrane dense structure, A_m is the permeation area of each element, $x_n[j]$ is the feed composition entering each cell, $y_n[j+1]$ is the permeate composition leaving each element. Via employment of the succession of states methodology, the flow rates in the retentate end, $V_R[\mathrm{j}+1]$, flow rate in the permeate sides, $V_P[\mathrm{j}+1]$, and retentate composition, $x_n[\mathrm{j}+1]$, that are output parameters for a designated membrane element, which would be consequently adapted as input conditions for the neighbouring membrane cell, are computed according to Eq. (4), Eq. (5) and Eq. (6).

$$V_R[\mathrm{j}+1] = V_R[\mathrm{j}] - \Delta V \quad (4)$$

$$V_P[\mathrm{j}+1] = V_P[\mathrm{j}] + \Delta V \quad (5)$$

$$x_n[\mathrm{j}+1] = \left(V_R[\mathrm{j}] x_n[\mathrm{j}] - \Delta V_n \right) / V_R[\mathrm{j}+1] \quad (6)$$

Finite Element Algorithm for Membrane Physical Aging

As mentioned earlier in the Introduction section, the thickness dependent physical aging within thin polymeric membrane films can be rationalized through a dual mode mechanism, which forms the basis of the mathematical model in present work. Several assumptions are as the following [2]:

i) The lost of free volume through lattice contraction mechanism is terminated when it reaches a glassy value, f_g. Subsequently, the lattice contraction mode no longer dominates and is governed by the vacancy diffusion theory,

ii) The lost of free volume via vacancy diffusion is symmetrical about the middle of a membrane sample along its thickness dimension.

Expression for the fractional free volume characterizing the diffusion mechanism, $f_D(x,t)$, which has been derived via separation of differential equation by additive $\left(f_D(x,t) = Q(x) + R(t) \right)$ [6, 7], has been adopted in Eq. (7).

$$f_D(x,t) = f_0 + \frac{1}{\beta_D} \ln \frac{8\alpha_D \exp\left(\beta_D \left(f_e + f_0 - f_g\right)\right)t + l^2 - 4x^2}{8\alpha_D \exp\left(\beta_D \left(f_{0g}\right)\right)t + l^2 - 4x^2} \quad (7)$$

α_D and β_D are the constants dependent upon the polymeric material, t is the aging time, x is the depth within the membrane matrix, l is the sample thickness, f_0, f_e and f_g correspond to the initial, equilibrium and bulk state fractional free volume that discriminates the incipient point for shift in dominancy from lattice contraction to vacancy diffusion. Then, Eq. (7) is integrated in a finite element algorithm along the polymeric film thickness, in which it is partitioned into predefined slices of membrane entity, N, that contains a varying response to aging at a particular time. Thereby, the average fractional free volume by vacancy diffusion from interior to surface of a polymeric membrane at a particular time, $\overline{f_D(t)}$, can be calculated through Eq. (8).

$$\overline{f_D(t)} = \frac{\sum_{n=1}^{N} f_D\left(nl/(2N), t\right)}{N} \quad (8)$$

Whereby n is the count parameter that characterizes the location of each membrane entity along the thickness within a membrane film ($n=1$ denotes the centre while $n=N$ corresponds to the surface). As for the lattice contraction mechanism, the fractional free volume has been calculated based upon Struik self retarding model [8] in current study, such as that provided in Eq. (9).

$$\frac{\partial \delta f_{LC}(t)}{\partial t} = -\frac{\partial f_{LC}(t)}{\tau_\infty \exp\left(-\gamma \delta f_{LC}(t)\right)} \quad (9)$$

In Eq. (9), $\delta f_{LC}(t)$ is the time dependent free volume departure from f_g, $\left(\delta f_{LC}(t) = f_{LC}(t) - f_g\right)$, which characterizes the driving force for lattice contraction mechanism, τ_∞ is the relaxation time at equilibrium while γ characterizes sensitivity of the relaxation time to the excess free volume. Eq. (9) has been solved analytically adopting the integral exponential function in Eq. (10).

$$Ei\left[-\gamma\left(f_{LC}(t) - f_g\right)\right] - Ei\left[-\gamma\left(f_{LC}(t) - f_0\right)\right] = t/\tau_\infty \quad (10)$$

Finally, the total fractional free volume at a particular aging time, $f(t)$, which is comprised of the vacancy diffusion and lattice contraction terms, is provided in Eq. (11).

$$f(t) = f_0 - \left(f_0 - \overline{f_D(t)}\right) - \left(f_0 - f_{LC}(t)\right) \quad (11)$$

The permeability at time, t, is modelled according to Eq. (12),

in which it is widely accepted to be an exponential function of the fractional free volume [9].

$$P(t) = a\exp(bf(t)) \quad (12)$$

Whereby a and b are material constants.

Model Validation

Accuracy of the succession of states describing separation mechanism of the cocurrent flow membrane has been verified through published data by Tranchino *et al.* (1989) [10], while applicability of the finite element algorithm describing physical aging has been validated with experimental data of Polysulfone (PSF) films by Rowe *et al.* (2011) [1] . General volumetric parameters obtained from experimental measurement that are adopted as input parameters for model validation are provided in Table 1. The model validation is provided in Figure 1, whereby the accuracy has been demonstrated through the small Mean Absolute Percentage Error (MAPE) value.

Table 1: Volumetric parameters of PSF film

Volumetric parameter	Value	Reference
Occupied volume of polymer, v_0 (cm^3/ g)	0.6903	[11]
Bulk density, ρ_b (g/ cm^3)	1.2400	[12]
Initial specific volume, v_i (cm^3/ g)	0.8110	[12]
Equilibrium specific volume, v_e (cm^3/ g)	0.7730	[12]
Initial fractional free volume, $f_0 = (v_i - v_0)/v_i$	0. 1488	[9]
Equilibrium fractional free volume, $f_e = (v_e - v_0)/v_e$	0. 1070	[9]
Glassy fractional free volume, $f_g = 1\text{-}\rho_b v_0$	0. 1440	[2]

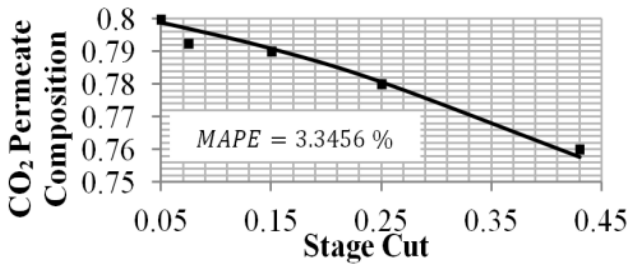

(a)

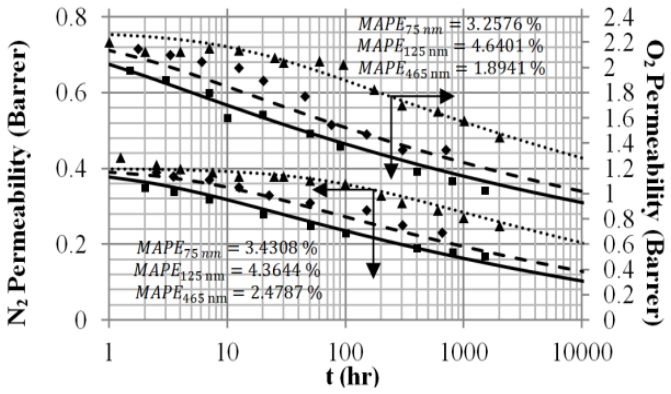

(b)

Figure 1: Model validation for (a) separation of cocurrent membrane by Tranchino, *et al.*, (1989); p_h / p_l = 405/ 101 kPa; $x_{F,CO_2} / x_{F,CH_4}$ = 60/ 40 %; P_{CO_2} / P_{CH_4} = 9.44/ 2.63 GPU; A_m = 20.78 cm^2 (b) Aged O_2 and N_2 permeability in PSF polymeric membrane films with varying thicknesses of 75 nm (■), 125 nm (◆) and 465 nm (▲) with simulation results of 75 nm (—), 125 nm (-------) and 465 nm (…….)

O_2 parameter: $\tau_\infty = 2.45\times10^{9}$; $\gamma = 500$; $\alpha_D = 7.5\times10^{-30.5}$; $\beta_D = 450$; $a = 0.006$; $b = 40$

N_2 parameter: $\tau_\infty = 3\times10^{9}$; $\gamma = 1500$; $\alpha_D = 9\times10^{-47.5}$; $\beta_D = 700$; $a = 0.0000325$; $b = 65$

Simulation and Optimization of Gas Separation

To evaluate effect of membrane thicknesses with consideration of physical aging to the separation performance of O_2/ N_2 separation, a single membrane module is simulated with feed gas of 500000 cm^3 (STP) s^{-1} flow rate and 50 bar pressure while the permeate stream is maintained at 1 bar [13]. Feed gas containing 21% O_2 and 79% N_2 is simulated, corresponding to the industrial application of air purification. The membrane material is assumed to be the commonly used PSF with its characteristic as demonstrated in previous section. For each membrane thickness, the membrane area is altered to ensure the product quality achieves the minimal requirement of 35% O_2 composition in permeate stream [14]. In addition, to incorporate effect of physical aging, the time dependent membrane permeability over the duration of 1 year has been employed with the same membrane area plotted for a particular membrane thickness. The simulation results are demonstrated in Figure 2, whereby Figure 2 (a) depicts the effect of membrane thicknesses to membrane area based on initial membrane performance, while Figure 2 (b) shows the effect of physical aging to the recovered oxygen over the course of a 1 year aging period.

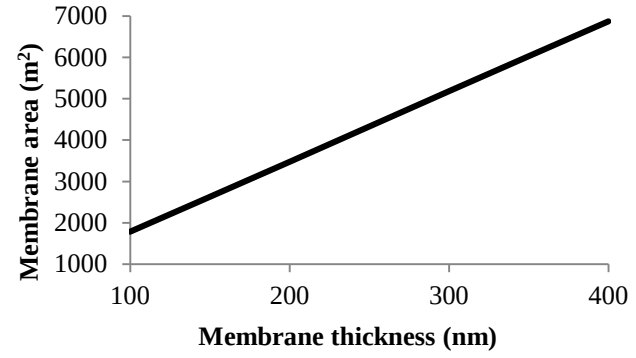

(a)

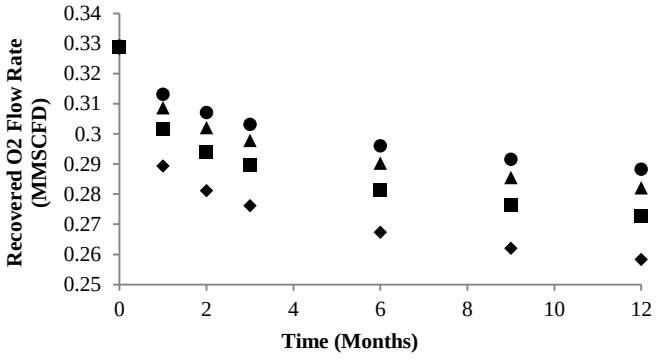

(b)

Figure 2: Effect of membrane thicknesses with consideration of physical aging to a) membrane area requirement and b) flow rate of recovered oxygen

[100 nm (◆), 200 nm (■), 300 nm (▲) and 400 nm (●)]

In Figure 2 (a), it is found that the smallest membrane thickness (100 nm) requires the smallest membrane area to achieve the designated product specification as compared to thickest membrane (400 nm) by 3.85 times. Such observation can be rationalized as a smaller resistance through the barrier that controls the relative rate of transport of various species, which constitutes to larger permeation to remove impurities under a smaller membrane area requirement [5, 15]. From Figure 2 (b), it is depicted that the oxygen flow rate recovered in the permeate stream decreases over time attributed to physical aging, whereby the volume relaxation within the glassy polymeric membrane contributes to reduction of free volume that confines the gas permeability [16]. Moreover, it is also demonstrated that the recovery depletes more significantly for the thinner membrane. In current study, the percentage product recovery after 1 year aging for the 100 nm, 200 nm, 300 nm and 400 nm PSF membranes are 21.35%, 17.06%, 14.27% and 12.39%. This phenomenon is attributed to the accelerated aging in thinner membrane film, which is consistent with the notion of enhanced mobility at the polymer surface for thin structure [17].

Therefore, it is depicted that albeit the inherent higher permeance of thinner polymeric membrane, making it a highly sought after structure as compared to its bulk counterpart, the thinner membrane also exhibits drawback of accelerated physical aging, which contributes to a higher fluctuation to cater a typical membrane system. In order to determine the optimum specification, the gas processing cost (GPC) per MSCF of product must be minimal over the duration of aging. The membrane cost for air separation has been approximated to be \$75/ m^2 [14]. As for the total oxygen flow rate recovered in the permeate stream, it has been determined by computing area under the curve as depicted in Figure 2 (b) via employment of numerical integration (trapz) in Matlab® 2013. The GPC of different membrane thicknesses during the course of 1 year aging has been determined, as illustrated in Figure 3. By differentiating the correlation obtained in Figure 3, the membrane specification that constitutes to minimum GFC per MSCF product from this study is determined to be 174 nm.

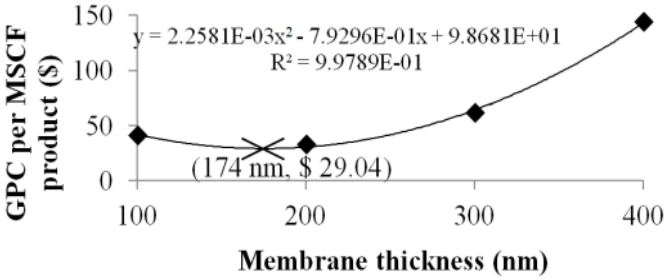

Figure 3: GPC per MSCF product under different membrane thicknesses

CONCLUSION

In this work, the physical aging phenomenon has been integrated within the separation mechanism of membrane, which has been validated with published experimental results. The mathematical model has been adopted to evaluate the effect of membrane thicknesses with consideration of physical aging to the separation performance of O_2/ N_2 gas separation. Based on the study's findings, it is concluded that despite the inherent higher permeance characteristic in thinner polymeric membrane, which contributes to smaller membrane area requirement to treat a given process stream, the thinner membrane also exhibits drawback of accelerated physical aging. The accelerated physical aging constitutes to faster deterioration of membrane performance and hence higher rate of process instability. Via incorporation of a simple process economics study, it is found that the optimal membrane thickness after 1 year aging is 174 nm. In future work, it is deemed important to implement a comprehensive evaluation with consideration of other auxiliary equipment in gas processing plant, e.g. compressor and heat exchanger, cost of product lost as well as variable operating and maintenance cost under varying membrane operating parameters and

design configurations to quantify the effect of physical aging to membrane separative performance in a more precise manner.

ACKNOWLEDGEMENT

This work is done with the financial support from Universiti Teknologi PETRONAS.

REFERENCES

[1] B. W. Rowe, *et al.*, "Gas-separation Problems with Membranes," in *Physical Aging of Membranes for Gas Separations. În: Membrane Engineering for the Treatment of Gases* vol. 1, ed Cambridge: Royal Society of Chemistry, 2011, pp. 58-83.

[2] M. S. McCaig, *et al.*, "Effect of film thickness on the changes in gas permeability of a glassy polyarylate due to physical aging Part II. Mathematical model," *Polym.*, vol. 41, pp. 639-648, 2000.

[3] S. S. M. Lock, *et al.*, "Mathematical Modeling of Thickness Dependent Physical Aging in Polymeric Membranes," *Key Eng. Mater.*, vol. 701, pp. 275-280, 2016.

[4] M. J. Thundyil and W. J. Koros, "Mathematical modeling of gas separation permeators — for radial crossflow, countercurrent, and cocurrent hollow fiber membrane modules," *J. Membr. Sci.*, vol. 125, pp. 275-291, 1997/03/19/ 1997.

[5] S. S. M. Lock, *et al.*, "Modeling, simulation and economic analysis of CO2 capture from natural gas using cocurrent, countercurrent and radial crossflow hollow fiber membrane," *Int. J. Greenh. Gas Control* vol. 36, pp. 114-134, 2015.

[6] A. W. Thornton, *et al.*, "New relation between diffusion and free volume: I. Predicting gas diffusion," *J. Membr. Sci.*, vol. 338, pp. 29-37, 2009.

[7] A. W. Thornton, *et al.*, "New relation between diffusion and free volume: II. Predicting vacancy diffusion," *J. Membr. Sci.*, vol. 338, pp. 38-42, 8/10/ 2009.

[8] L. C. E. Struik, "Physical Aging in Amorphouse Glassy Polymers," *Annals of the New York Academy of Sciences*, vol. 279, pp. 78-85, 1976.

[9] J. Y. Park and D. R. Paul, "Correlation and prediction of gas permeability in glassy polymer membrane materials via a modified free volume based group contribution method," *J. Membr. Sci.*, vol. 125, pp. 23-39, 1997.

[10] L. Tranchino, *et al.*, "Gas Separation in a Membrane Unit: Experimental Results and Theoretical Predictions," *Sep. Sci. Techol.*, vol. 24, pp. 1207-1226, 1989/11/01 1989.

[11] A. Bondi, *Physical properties of molecular crystals, liquids and glasses*. New York [etc.]: John Wiley & Sons, 1968.

[12] Y. Huang, *et al.*, "Physical aging of thin glassy polymer films: Free volume interpretation," *J. Membr. Sci.*, vol. 277, pp. 219-229, 2006.

[13] A. Nakao, *et al.*, "Modeling of Flowcharts of Permeation Through Membranes for Removal of CO2 of Natural Gas," *Comput. Aided Chem. Eng.*, vol. 27, pp. 1875-1880, 2009/01/01/ 2009.

[14] R. Jain, "Method for economic evaluation of membrane-based air separation," *Gas Sep. Purif.*, vol. 3, pp. 123-127, 1989/09/01/ 1989.

[15] S. S. M. Lock, *et al.*, "Effect of recycle ratio on the cost of natural gas processing in countercurrent hollow fiber membrane system," *J. Ind. Eng. Chem.* , vol. 21, pp. 542-551, 2015.

[16] J. Exposito, *et al.*, "Study of Polymer Material Aging by Laser Mass Spectrometry, UV-Visible Spectroscopy, and Environmental Scanning Electron Microscopy," *Res. Lett. Phys. Chem.*, vol. 2007, 2007.

[17] B. W. Rowe, *et al.*, "Physical aging of ultrathin glassy polymer films tracked by gas permeability," *Polym.*, vol. 50, pp. 5565-5575, 11/3/ 2009.